



Influence of paper thickness on the electrochemical performances of graphene papers as an anode for lithium ion batteries

Yuhai Hu^a, Xifei Li^a, Dongsheng Geng^a, Mei Cai^b, Ruying Li^a, Xueliang Sun^{a,*}

^a Department of Mechanical and Materials Engineering, Faculty of Engineering, The University of Western Ontario, London, Ontario, N6A 5B7 Canada

^b General Motors R&D Center, Warren, MI 48090-9055, USA

ARTICLE INFO

Article history:

Received 12 September 2012

Received in revised form

17 December 2012

Accepted 25 December 2012

Available online 2 January 2013

Keywords:

Graphene

Graphene paper

Lithium ion battery

Electrochemical energy storage

Freestanding

ABSTRACT

This paper focuses on an understanding of the influence of paper thickness on the electrochemical performances of graphene papers as an anode for lithium ion batteries. Three types of graphene papers, with thickness of ~ 1.5 , 3 and $10 \mu\text{m}$, respectively, were fabricated by vacuum-assisted filtration of reduced graphene nanosheets suspended in water. These papers deliver evidently different lithium storage capacities, with thinner papers always outperform thicker ones. The $1.5 \mu\text{m}$ paper gives rise to initial reversible specific capacities (the first 10 cycles) of $\sim 200 \text{mAh g}^{-1}$ at a current density of 100mA g^{-1} , while the $10 \mu\text{m}$ paper only presents $\sim 80 \text{mAh g}^{-1}$ at a current density of 50mA g^{-1} . After 100 cycles, a specific capacity of $\sim 180 \text{mAh g}^{-1}$ is retained for the $1.5 \mu\text{m}$ paper; in contrast, only $\sim 65 \text{mAh g}^{-1}$ remains for the $10 \mu\text{m}$ paper. The capacity decline with the paper thickness is associated with the dense restacking of graphene nanosheets and a large aspect ratio of the paper. The effective Li^+ diffusion distance in graphene paper is mainly controlled by the thickness of the paper, and the diffusion proceeds mainly in in-plane direction, cross plane diffusion is restrained. As such, the effective contact of graphene nanosheets with electrolyte is limited and the efficiency of carbon utilization is very low in the thick papers.

© 2013 Elsevier Ltd. All rights reserved.

1. Introduction

Potential application of graphene in electrochemical energy conversion and storage has drawn increasing interest rapidly [1–3]. The incorporation of graphene into traditional electrode materials for lithium ion batteries (LIBs), i.e., forming hybrid nanocomposites, can improve battery performance [4–11]. Meanwhile, graphene has also been used directly as anode for LIBs and exhibits intriguing performance [12–17]. Therefore, the assembly of graphene nanosheets (GNS) into thin films and papers is an attractive subject [18–23]. Graphene papers are highly freestanding and usually flexible. The papers can be easily fabricated using directed-flow assembly method [24]. The introduction of freestanding graphene paper into lithium ion battery assembly offers several advantages. Such a design generally requires fewer steps in anode fabrication and battery assembly, with potential to eliminate electric conductors and polymer binders that are used in conventional powder-based anodes fabrication. Graphene paper possesses equal or even higher flexibility than that of metal foils do but has much lower mass, which renders the fabrication of thin film battery possible.

Research on graphene paper as anodes for LIBs is developing very rapidly [18–20,22]. However, the existing work is inconsistent and most of them indicated that graphene paper could not offer specific capacities equal to or higher than those of graphene powders. Wallace's group firstly reported graphene paper as anode for LIBs [20]. A paper of $\sim 5 \mu\text{m}$ thickness presented a first discharge capacity of 582mAh g^{-1} . The capacity dropped to $\sim 95 \text{mAh g}^{-1}$ at the second cycle and then at a very slow pace in the following cycles. Their results were corroborated by Nguyen, et al., who fabricated a non-annealed graphene paper via hydrazine reduction of prefabricated graphene oxide paper and further used it as a binder-free alternative anode [22]. The graphene paper, which is $\sim 10 \mu\text{m}$ thick, exhibited a charge-discharge profile that closely resembles those reported for polymer-bound graphene-based anodes while maintaining excellent cyclability over 70 charge-discharge cycles. Significant increases in the reversible capacity (from 84 to 214mAh g^{-1}) were observed when the current rate was decreased from 50 to 10mA g^{-1} . They assumed that there are possible kinetic barriers to Li ion diffusion as a result of the layered structure of the graphene paper. Most recently, Hyeokjo Gwon, et al., compared battery performances of graphene paper and graphene powder [19]. Their graphene paper, about $2 \mu\text{m}$ thick, obviously outperformed their graphene powder. At a rate of 1C (372mA g^{-1}), the capacity achieved $\sim 200 \text{mAh g}^{-1}$ and increased steadily in the following cycles; on the other hand, the capacity of graphene powder was only 160mAh g^{-1} and decreased steadily. This is interesting

* Corresponding author. Tel.: +1 519 661 2111x87759.

E-mail address: xsun9@uwo.ca (X. Sun).

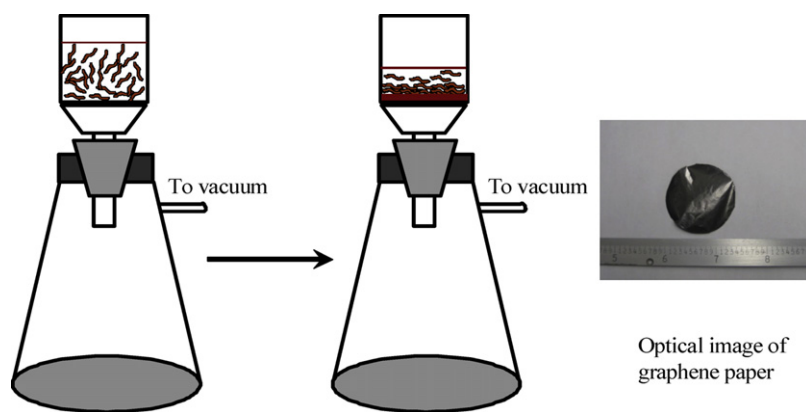


Fig. 1. Schematic diagram for the fabrication of graphene paper through vacuum assisted filtration of GNS dispersion and a photograph of as-prepared graphene paper.

because usually, graphene powder, due to its high surface area, possess much higher capacity than graphite does ($\sim 372 \text{ mAh g}^{-1}$) [14–17]. Obviously, aside from improving the energy capacities of graphene paper, it is also necessary to explore the intrinsic factors that mediate the battery performance of graphene paper. But, such research has not been carried out before.

In this paper, we systematically studied electrochemical performances of graphene papers as anodes for LIBs, focusing on understanding of the influence of paper thickness on the lithium ion storage capacities of the papers. The study on three types of graphene paper reveals that (1) the decline in capacities with increase of paper thickness is due to restack of GNS and a large aspect ratios of the papers; (2) the effective diffusion distance of Li in graphene paper is controlled by the thickness of the paper, and the diffusion mainly proceeds in in-plane direction, cross-plane diffusion is restrained; and (3) the graphene paper is expected to have potential application in lithium ion batteries.

2. Experimental

2.1. Fabrication of graphene paper

Graphene paper was fabricated by vacuum assisted filtration of GNS dispersion. Typically, graphite oxide was synthesized through oxidation of graphite flakes with KMnO_4 , NaNO_3 , and H_2SO_4 using a modified Hummers method [25]. As synthesized graphite oxide was dispersed in deionized water to give rise to a 0.5 mg ml^{-1} suspension, and was then exfoliated by ultrasonication for 1 h. The obtained suspension was centrifuged at 5000 rpm for 15 min to obtain a homogeneous graphene oxide dispersion. For reduction, the dispersion was diluted to 0.25 mg ml^{-1} and was adjusted to $\text{pH} = 10$ with ammonia solution. Hydrazine water solution (35%)

was added into the dispersion and was stirred thoroughly at room temperature. The weight ratio of hydrazine to GO is set to be about 2:1. The dispersion was then put into an oil bath of 90°C , and the reaction was allowed to proceed for 2 h. Graphene paper was made by vacuum-assisted filtration of the resulting dispersion through an Anodisc membrane filter (47 mm diameter, $0.2 \mu\text{m}$ pore size; Whatman), followed by air drying for 24 h at room temperature and peeling from the filter. Thickness of the paper was tuned by adjusting the amount of the GNS dispersion. The whole process is schematically shown in Fig. 1. Before spectroscopic and electrochemical characterization, the graphene papers were mildly annealed in Ar-H_2 (10% H_2) atmosphere at 800°C for 2 h for additional deoxygenation. A photograph of the as-fabricated graphene paper in this study is shown in Fig. 1.

2.2. Characterization of graphene papers

Morphologies of GNS and graphene papers were characterized using a field emission scanning electron microscope (Hitachi S-4800) and transmission electron microscope (Philips CM10). Raman spectra were obtained on a HORIBA Scientific LabRAM HR Raman spectrometer system equipped with a 532.4 nm laser as the exciting radiation source. The system is also equipped with an optical microscope so as to generate confocal signals. To obtain charge-discharge profiles and cycle performance data, the graphene papers were used directly as an anode and were assembled in a CR 2032-type coin cell configuration. A lithium foil was used as a counter electrode. Electrolyte was composed of 1 M LiPF_6 salt dissolved in a solution consisting ethylene carbonate, diethyl carbonate, ethyl methyl carbonate (1:1:1 in volume). Charge-discharge characteristics were tested galvanostatically in a voltage range of 0.01–3.0 V (vs. Li^+/Li) at a desired current rate

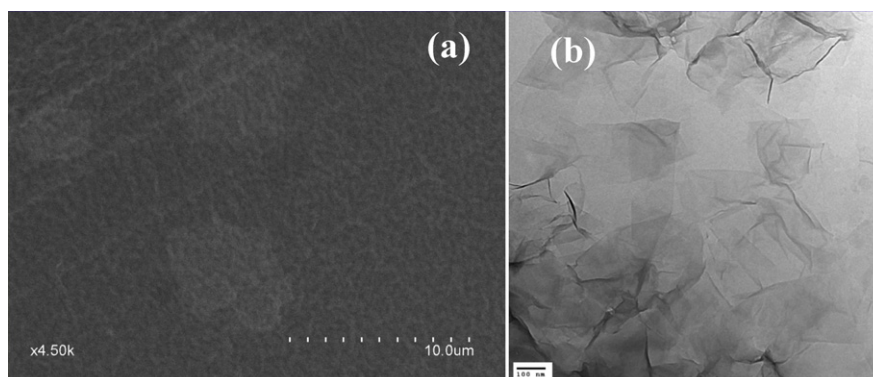


Fig. 2. (a) SEM and (b) TEM of reduced GNS before paper fabrication.

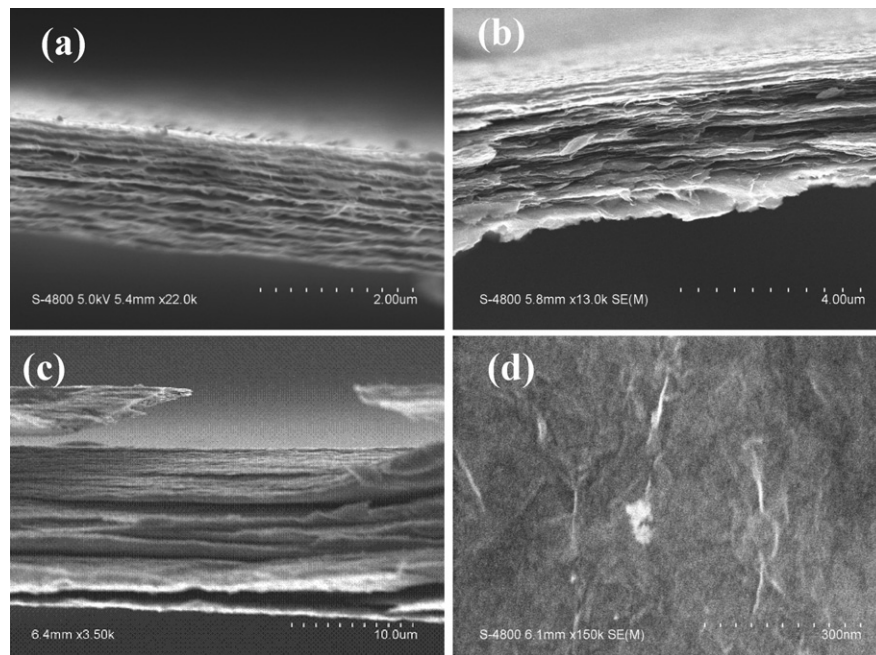


Fig. 3. SEM images of graphene papers: (a–c) cross sections of GP-I, GP-II and GP-III, respectively; (d) top view of GP-III.

using an Arbin BT-2000 Battery Test System. Cyclic voltammetry (CV) tests were performed on a versatile multichannel potentiostat 3/Z (VMP3) at a scan rate of 0.1 mV s^{-1} over a potential range of $0.01\text{--}3.0 \text{ V}$ (vs. Li^+/Li).

3. Result and discussion

3.1. Morphologies of GNS and graphene papers

The properties of a graphene paper, e.g., mechanical strength and electric conductivity, are intimately related to those of GNS (e.g., doping atoms, functionalizing groups and defects) and their assembly. Usually, under the assistant of high vacuum, large surface size and thin GNS give rise to graphene papers with high mechanical strength and electric conductivity [24]. Thicker paper is highly freestanding and flexible and therefore, is generally more macroscopically processable. SEM and TEM images of the GNS before paper assembly are shown in Fig. 2. The GNS are with sizes of $\sim 5 \mu\text{m}$ or smaller (Fig. 2(a)). TEM image exhibits transparent characteristic of the GNS, indicating they are composed of only thin graphene. HRTEM image confirms most of the resultant nanosheets consist of ≤ 7 layers with thickness of about 4 nm , as shown in Fig. S1. In this study, three types of graphene papers were fabricated following a same procedure. Cross sections of these papers are shown in Fig. 3. The papers have obviously different thickness, i.e., $\sim 1.5 \mu\text{m}$ (GP-I) in Fig. 3(a), $\sim 3 \mu\text{m}$ (GP-II) in Fig. 3(b) and $\sim 10 \mu\text{m}$ (GP-III) in Fig. 3(c), respectively. However, structures of the three papers are similar, possessing a layered structure through the entire cross section, a characteristic of graphene paper from vacuum-assisted filtration [20,22]. Surface morphology of the papers was also interrogated. Shown in Fig. 3(d) is the SEM image of the GP-II, which reveals an undulating morphology. These are highly consistent with those reported previously [20,22]. Moreover, the three papers in this study are highly freestanding and flexible. They can be bent to any angle, as shown in Fig. S2.

3.2. Electrochemical characterization of the graphene papers

Electrochemical properties of the papers were first characterized using cycle voltammetry (CV) method. The papers were used

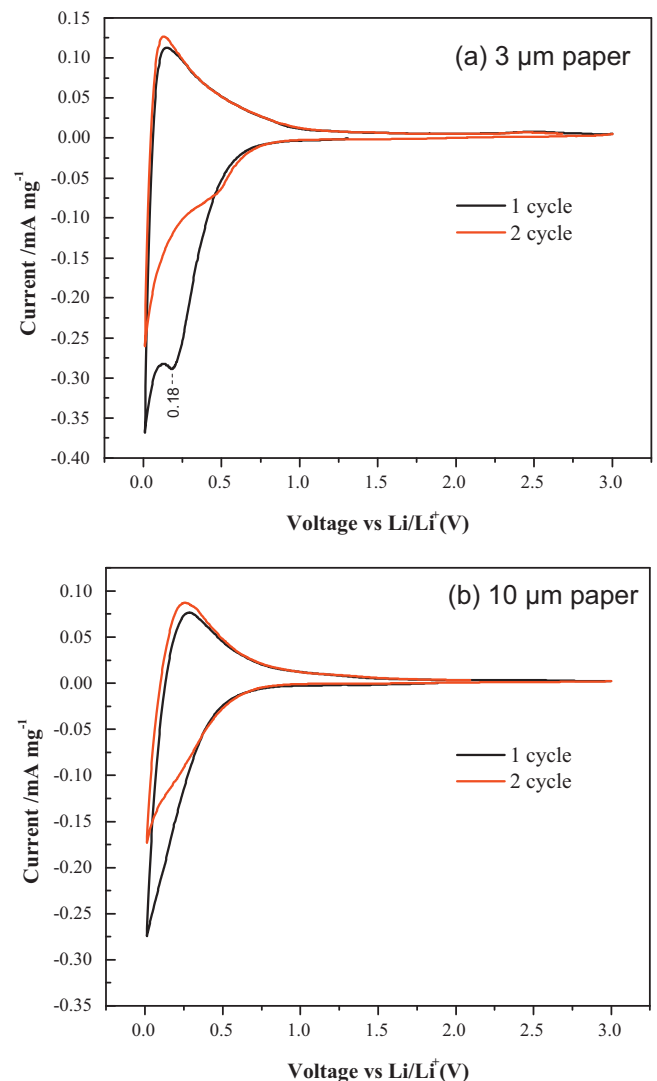


Fig. 4. Cyclic voltammetry curves of graphene papers.

as working electrodes in 1.0M LiPF₆ with lithium sheet as the counter and reference electrodes. The CV curves of the GP-II and GP-III shown in Fig. 4 revealed some insightful information on Li-GNS interactions. (1) For both papers, a peak, which results from Li intercalation into the carbon based anodes, was observed at close to 0V in both CV curves; and (2) CV behavior of the thinner paper is obviously different from that of the thicker one. As shown in Fig. 4(a), the first cycle of the GP-II electrode gives a predominant peak located at ~0.18V. Such a peak was also assumed to be related to intercalation of lithium into the graphene layers due to the structural defects in some basal planes of carbon nanosheets in the graphene paper, like the disordered carbon material [26]. This peak disappears in the second cycle as a result of the isolation between the anodes and electrolyte due to the dense SEI film that has been established on the surface of the anodes in the first discharge [17]. On the other hand, such peaks are not discernable in the curves of GP-III, for which the CV curves are similar to that of graphite reported previously in the voltage range lower than 0.6V [20]. Accordingly, it can be suggested that the CV behavior of graphene paper is strongly dependent on the paper thickness, with the thicker graphene paper behaves similar to graphite while the thinner ones behave similar to graphene powder.

Battery performance of the three papers was tested in coin cell lithium ion batteries. The charge-discharge profiles of the GP-I and

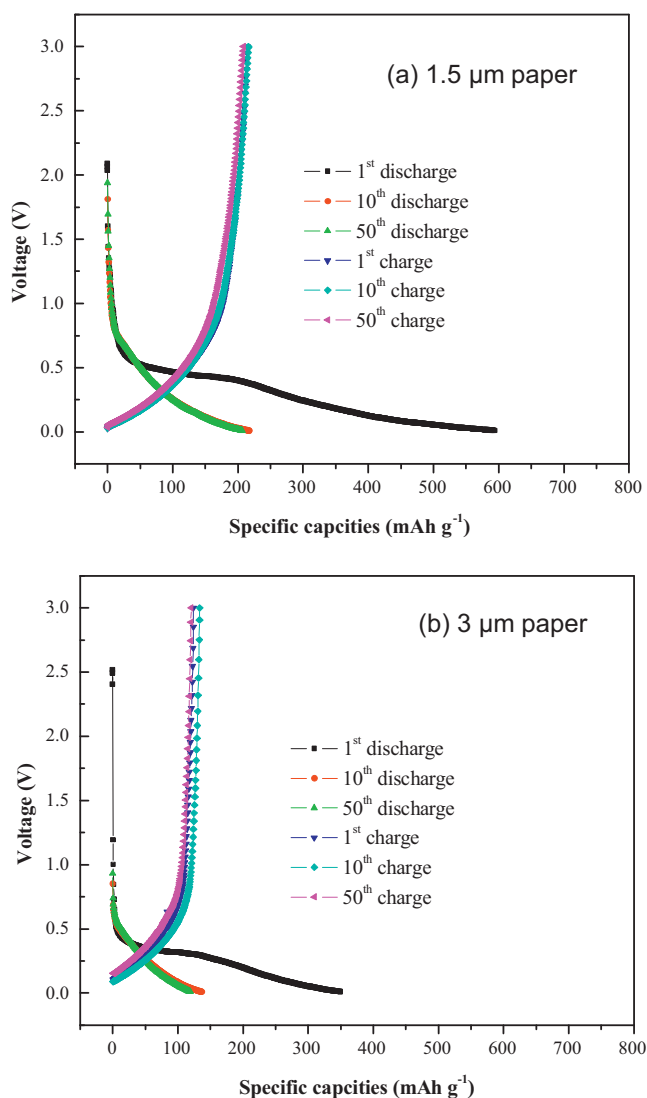


Fig. 5. Charge-discharge profiles of GP-I and GP-II.

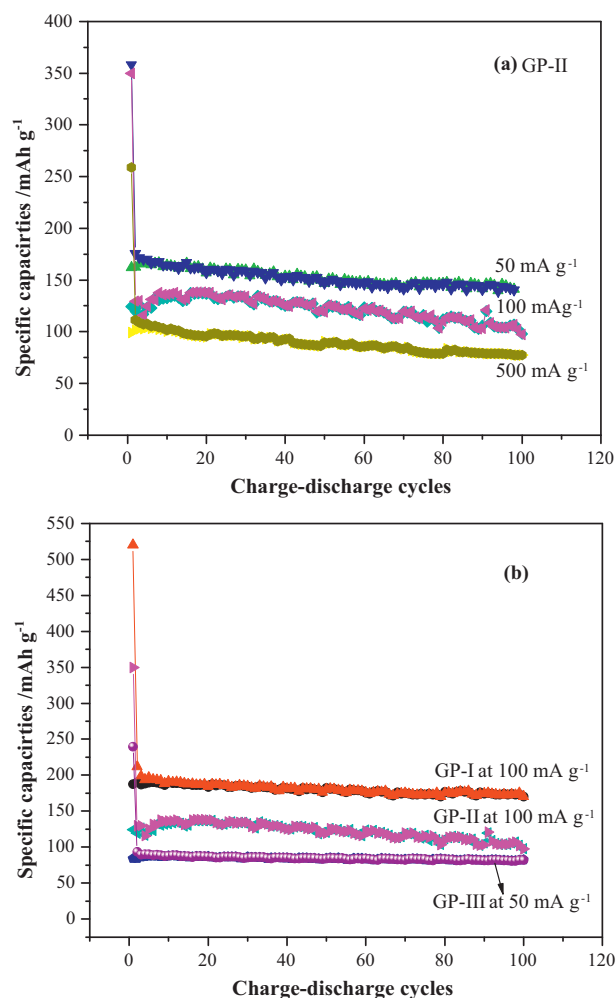


Fig. 6. Electrochemical characterization of graphene papers as anode: (a) charge-discharge cycles of GP-II tested at various current rates; (b) charge-discharge cycles of different graphene papers tested at 100 mA g⁻¹.

GP-II are shown in Fig. 5. On the first discharge, there is a plateau at ~0.5V for both types of papers. The plateau for the 1.5 μm paper is longer than that for the 3 μm paper, indicating that this step offer more capacity for the thinner paper. The plateau is not visible in the second and following cycles, suggesting that it might be associated with SEI formation, i.e., an irreversible process. Meanwhile, the capacities are much lower than that for the first cycle, and do not change greatly after 50 cycles. The charge process finishes below 0.8V. This feature is consistent with the CV curves. The capacities remain almost unchanged after 50 cycles. Cyclic performances of the papers, tested under various conditions, are shown in Fig. 6. Overall, irrespective of the current density and the paper thickness, much higher irreversible specific capacities are observed in the first discharge, e.g., ~540 mAh g⁻¹ for the GP-I at 100 mA g⁻¹. The reversible specific capacities are considerably lower than the first discharge capacity and decrease at a slow pace following charge-discharge cycles, which is a typical feature of graphene when used as anodes for lithium ion batteries and is consistent with previously published data [20,22]. The most intriguing information conveyed in this figure is that the performances of graphene papers are highly dependent on the paper thickness and the current density. For the GP-II, reducing current density always leads to increase in the reversible specific capacity. The reversible discharge capacities at 500 mA g⁻¹ are beyond 100 mAh g⁻¹ in the first 10 cycles and remain ~80 mAh g⁻¹ after 100 cycles. At 100 mA g⁻¹, the capacities

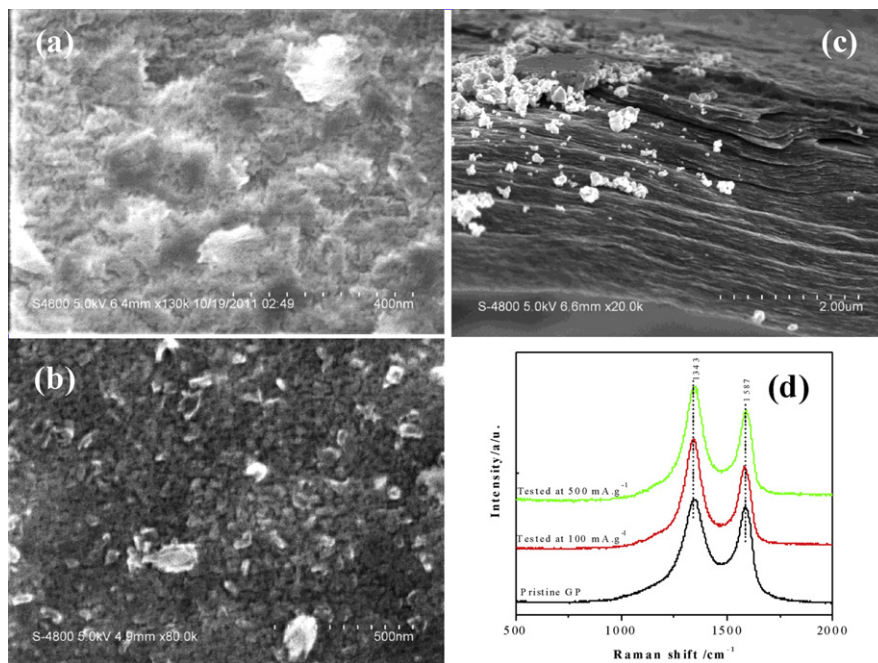


Fig. 7. SEM images and Raman spectra of GP-II after 100 charge-discharge cycles at different current rates: (a and b) top views of the paper tested at 100 and 500 mA g⁻¹, respectively; (c) cross section of the paper tested at 100 mA g⁻¹; (d) Raman spectra.

drop to ~ 105 from ~ 135 mAh g⁻¹; but at 50 mA g⁻¹, the capacities change from ~ 175 to ~ 145 mAh g⁻¹. These results prove that the battery performance of graphene paper is a kinetically related process. Moreover, thinner paper exhibits obviously higher capacities than thick one does. The GP-III, i.e., ~ 10 μ m, shows the lowest capacities among three papers, ranging from 80 to 70 mAh g⁻¹ at 50 mA g⁻¹; on the other hand, for the thinnest paper, i.e., the GP-I, the capacities are in the range from ~ 200 to ~ 175 mAh g⁻¹ at 100 mA g⁻¹. Following these, it can be concluded that thickness is a key factor that mediates the battery performance of a graphene paper as an anode; the thinner, the higher specific capacities.

3.3. Characterization of graphene papers after battery test

To get further insight of the changes in graphene papers resulting from Li intercalation and hence the electrochemical behaviors of the papers as anode, the papers were characterized using SEM and Raman after 100 charge-discharge cycles. Shown in Fig. 7 are the images of the GP-II after tests at 100 and 500 mA g⁻¹, respectively. Compared to the images of the untested papers shown in Fig. 3(b), significant changes in the morphology of the papers happen. At both current rates, the paper surface has smashed, and many carbon clusters are observed. Inside each cluster, there are many pores. More interestingly, the clusters are relatively smaller in the 500 mA g⁻¹ paper, with sizes of ~ 100 nm. Raman spectra collected on the surface of the tested papers are shown in Fig. 7(d). Evidently, D band was enhanced after test (I_D/I_G increases from 1.08 to 1.38 at 500 mA g⁻¹), but the Raman shifts of both peaks remain unchanged at both current rates. This suggests that more defect sites were created during the process of Li intercalation and deintercalation, i.e., graphene layer has smashed to some extent.

However, intercalation of Li does not proceed deeply into the paper. Image of the cross section of the tested GP-II (Fig. 7(c)) unambiguously reveals that cracking of the paper took place mostly on the surface and the whole structure of the paper persists. This is further corroborated by Raman mapping on the cross section of

the paper. For this purpose, the tested paper was cut into a desired piece and the cross section of the fresh cut was characterized. The spectra of the mapping are shown Fig. S3. The insertion shows the photograph of the cross section. There are evident spectral changes following the mapping. The strongest signals appear in the scale from 4.3 to 7.5 μ m, which is close to the thickness of the paper. The intensity fluctuation is mainly due to the unevenness of cross section. Our Raman system is confocal, for which the signal intensity is highly dependent on the relative position between lens and specimen, in other word, focus. The intensity difference between D band and G band are obviously different at different positions. As shown in Fig. S4, the D band at 4.3 and 7.5 μ m are much stronger than those at 5.8 and 6.6 μ m, i.e., there are more defect sites on the surface of the paper than in the middle. This, in turn, suggests that the GNS in the middle area of the paper are not accessible to electrolyte (Li) and therefore, are not or less disturbed.

Following all these results, the decline in capacity with paper thickness can be explained in terms of restack of GNS and low surface areas of the papers. As well known, in graphene paper, GNS are layered with their planes parallel to the paper surface. The restack is so good that layer-layer distance (d -spacing) is ~ 0.379 nm, which is close to a d -spacing of 0.336 nm for graphite [20]. Post-annealing renders the d -spacing even smaller. Such an assembly offers the paper high mechanical strength, electric conductivity (interface resistances is reduced considerably, even though still higher than that of graphite), and flexibility, making macroscopic process of graphene feasible. On the other hand, as a result of such a dense assembly, many unique properties that individual GNS possess, such as high specific surface area (or defect sites) and peculiar electron transport behaviors, are significantly diminished or even unavailable [27]. Consequently, in graphene paper, much less tunnels are available for electrolyte (Li) to diffuse into the bulk of the paper. Notice cross-plane diffusion of Li⁺ in graphene is not energy favorable [28]. The diffusion of Li⁺ in graphene paper proceeds mainly in in-plane direction but not in the cross-plane direction. Under such situation, (1) the effective diffusion distance is mainly controlled by the thickness of the paper, and (2) when tested at

a same current rate, not all the carbon (actually, GNS) has been reached by Li in thick graphene paper; in other word, efficiency of carbon utilization is lower, accounting for the lower *specific capacity* in thicker paper.

It is true that the performances of bulk graphene films do not compete with conventional porous carbon materials for massive use in energy storage devices. Note that graphite is an assembly of graphene but attributes of every single sheet is not realized as a consequence of the dense packing and significant reduction of defect sites. Shen and Raj, in their study of silicon-oxycarbide (SiCO) based thin film anodes for lithium ion batteries [29], found that battery performance is highly dependent on the thickness of the thin films, and films with a thickness of less than approximately 1 μm have much higher performance. A 0.5 μm thick thin film exhibited capacities higher than 1000 mAh g^{-1} , while 5.5 μm film only provided <150 mAh g^{-1} . They suggested that the diffusion of Li into the SiCO film is likely to be controlled by diffusion parallel to plane of the film. Moreover, it is also found that when used as electrodes for supercapacitors, physically separated graphene sheets that are vertically grown on a metal substrate show an exceptional frequency response. This result, however, has been considered difficult to realize in porous bulk graphene films due to the increased difficulty of ions diffusion caused by intersheet aggregation [27,30].

Finally, it is worth emphasizing that in term of energy efficiency, high specific capacities can be explored if the thickness of graphene paper goes down to nanometer scale (i.e., <1 μm). However, such a thin paper is hardly maintained as freestanding and therefore is difficult for macroscopic processing if there are no suitable substrates. This is a topic of interest in graphene thin films, which is not the primary purpose of this study. It remains an interesting topic but a challenge to obtain freestanding graphene papers possessing both high mechanical strength and high lithium storage capacities [23,31,32]. We are also working on this.

4. Conclusion

Electrochemical performances of freestanding graphene papers as anodes for lithium ion batteries are highly dependent on the paper thickness. Thinner papers always offer higher specific capacities than thicker one does. The decline in capacity with increased paper thickness was attributed to densely restacking of graphene nanosheets and low surface area of the paper. The effective diffusion distance of Li ions in graphene paper is mainly controlled by the thickness of the paper, and the diffusion of Li ions in graphene paper proceeds mainly in in-plane direction rather than in the cross-plane direction. Efficiency of carbon utilization is therefore very low for thick papers. It is expected that freestanding graphene paper has potential application in lithium ion batteries.

Acknowledgements

This research was supported by the Natural Science and Engineering Research Council of Canada (NSERC), General Motors, Canada Research Chair (CRC) Program, Canadian Foundation for Innovation (CFI), Ontario Research Fund (ORF) and the University of Western Ontario.

Appendix A. Supplementary data

Supplementary data associated with this article can be found, in the online version, at <http://dx.doi.org/10.1016/j.electacta.2012.12.106>.

References

- [1] D.A.C. Brownson, D.K. Kampouris, C.E. Banks, An overview of graphene in energy production and storage, *Journal of Power Sources* 196 (2011) 4873.
- [2] S.J. Guo, S.J. Dong, Graphene nanosheet: synthesis, molecular engineering, thin film, hybrids, and energy and analytical applications, *Chemical Society Reviews* 40 (2010) 2644.
- [3] Y.Q. Sun, Q. Wu, G.Q. Shi, Graphene based new energy materials, *Energy & Environmental Science* 4 (2011) 1113.
- [4] S.M. Bak, K.W. Nam, C.W. Lee, K.H. Kim, H.C. Jung, X.Q. Yang, K.B. Kim, Spinel LiMn_2O_4 /reduced graphene oxide hybrid for high rate lithium ion batteries, *Journal of Materials Chemistry* 21 (2011) 17309.
- [5] J. Yao, X.P. Shen, B. Wang, H.K. Liu, G.X. Wang, In situ chemical synthesis of SnO_2 -graphene nanocomposite as anode materials for lithium-ion batteries, *Electrochemistry Communications* 11 (2009) 1849.
- [6] M. Zhang, D. Lei, X.M. Yin, L.B. Chen, Q.H. Li, Y.G. Wang, T.H. Wang, Magnetite/graphene composites: microwave irradiation synthesis and enhanced cycling and rate performances for lithium ion batteries, *Journal of Materials Chemistry* 20 (2010) 5538.
- [7] H.Y. Kim, S.W. Kim, J.Y. Hong, H.D. Lim, H.S. Kim, J.K. Yoo, K. Kang, Graphene-based hybrid electrode material for high-power lithium-ion batteries, *Journal Electrochemical Society* 158 (2011) A930.
- [8] X.F. Zhou, F. Wang, Y.M. Zhu, Z.P. Liu, Graphene modified LiFePO_4 cathode materials for high power lithium ion batteries, *Journal of Materials Chemistry* 21 (2011) 3353.
- [9] J. Yang, J. Wang, D. Wang, X. Li, D. Geng, G. Liang, M. Gauthier, R. Li, X. Sun, 3D porous LiFePO_4 /graphene hybrid cathodes with enhanced performance for Li-ion batteries, *Journal of Power Sources* 208 (2012) 340.
- [10] X.J. Zhu, Y. Zhu, S. Murali, M.D. Stoller, R.S. Ruoff, Reduced graphene oxide/tin oxide composite as an enhanced anode material for lithium ion batteries prepared by homogenous coprecipitation, *Journal of Power Sources* 196 (2011) 6473.
- [11] X. Li, X. Meng, J. Liu, D. Geng, Y. Zhang, M. Banis, Y. Li, R. Li, X. Sun, M. Cai, M. Verbrugge, Tin oxide with controlled morphology and crystallinity by atomic layer deposition onto graphene nanosheets for enhanced lithium storage, *Advanced Functional Materials* 22 (2012) 1647.
- [12] Y. Li, J. Wang, X. Li, D. Geng, M. Banis, R. Li, X. Sun, Nitrogen-doped graphene nanosheets as cathode materials with excellent electrocatalytic activity for high capacity lithium-oxygen batteries, *Electrochemistry Communications* 18 (2012) 12.
- [13] Y. Li, J. Wang, X. Li, D. Geng, R. Li, X. Sun, Superior energy capacity of graphene nanosheets for a nonaqueous lithium-oxygen battery, *Chemical Communications* 47 (2011) 9438.
- [14] E.J. Yoo, J.D. Kim, E. Hosono, H.S. Zhou, T. Kudo, I. Honma, Large reversible Li storage of graphene nanosheet families for use in rechargeable lithium ion batteries, *Nano Letters* 8 (2008) 2277.
- [15] P. Chen, H.H. Song, X.H. Chen, Electrochemical performance of graphene nanosheets as anode material for lithium-ion batteries, *Electrochemistry Communications* 11 (2009) 1320.
- [16] X.C. Xiao, P. Liu, J.S. Wang, M.W. Berbrugge, M.P. Balogh, Vertically aligned graphene electrode for lithium ion battery with high rate capability, *Electrochemistry Communications* 13 (2011) 209.
- [17] X. Li, D. Geng, Y. Zhang, X. Meng, R. Li, X. Sun, Superior cycle stability of nitrogen-doped graphene nanosheets as anodes for lithium ion batteries, *Electrochemistry Communications* 13 (2011) 822.
- [18] X. Zhao, C.M. Hayner, M.C. Kung, H.H. Kung, Flexible holey graphene paper electrodes with enhanced rate capability for energy storage applications, *ACS Nano* 5 (2011) 8739.
- [19] H. Gwon, H.S. Kim, K.U. Lee, D.H. Seo, Y.C. Park, Y.S. Lee, B.T. Ahn, S. Kang, Flexible energy storage devices based on graphene paper, *Energy & Environmental Science* 4 (2011) 1277.
- [20] C.Y. Wang, D. Li, C.O. Too, G.G. Wallace, Electrochemical properties of graphene paper electrodes used in lithium batteries, *Chemistry of Materials* 21 (2009) 2604.
- [21] A.L.M. Reddy, A. Srivastava, S.R. Gowda, H. Gullapalli, M. Dubey, P.M. Ajayan, Synthesis of nitrogen-doped graphene films for lithium battery application, *ACS Nano* 4 (2010) 6337.
- [22] A. Abouimrane, O.C. Compton, K. Amine, S.T. Nguyen, Non-annealed graphene paper as a binder-free anode for lithium-ion batteries, *Journal Physical Chemistry C* 114 (2010) 12800.
- [23] F. Liu, S. Song, D. Xue, H. Zhang, Folded structured graphene paper for high performance electrode materials, *Advanced Materials* 24 (2012) 1089.
- [24] D.A. Dikin, S. Stankovich, E.J. Zimney, R.D. Piner, G.H.B. Dommett, G. Evenenko, S.T. Nguyen, R.S. Ruoff, Preparation and characterization of graphene oxide paper, *Nature* 448 (2007) 457.
- [25] W.S. Hummers, R.E. Offeman, Preparation of graphitic oxide, *Journal of American Chemical Society* 58 (1958) 1339.
- [26] M.D. Levi, D. Aurbach, The mechanism of lithium intercalation in graphite film electrodes in aprotic media. Part 1. High resolution slow scan rate cyclic voltammetric studies and modeling, *Journal of Electroanalytical Chemistry* 421 (1997) 79.
- [27] X.W. Yang, J.W. Zhu, L. Qiu, D. Li, Bioinspired effective prevention of restacking in multilayered graphene films: towards the next generation of high-performance supercapacitors, *Advanced Materials* 23 (2011) 2833.

- [28] E. Pollak, B.S. Geng, K.J. Joen, I.T. Lucas, T.J. Richardson, F. Wang, R. Kostecki, The interaction of Li^+ with single-layer and few-layer graphene, *Nano Letters* 10 (2010) 3386.
- [29] J. Shen, R. Raj, Silicon-oxycarbide based thin film anodes for lithium ion batteries, *Journal of Power Source* 196 (2011) 5945.
- [30] J.R. Miller, R.A. Outlaw, B.C. Holloway, Graphene double-layer capacitor with ac line-filtering performance, *Science* 329 (2010) 1637.
- [31] R. Mukherjee, A.V. Thomas, A. Krishnamurthy, N. Koratkar, Photothermally reduced graphene as high-power anodes for lithium-ion batteries, *ACS Nano* (2012), <http://dx.doi.org/10.1021/nn303145j>.
- [32] X. Zhao, C.M. Hayner, M.C. Kung, H.H. Kung, In-plane vacancy-enabled high-power Si-graphene composite electrode for lithium-ion batteries, *Advanced Energy Materials* 1 (2011) 1079.